ISSN 2616-5775 Vol. 9, Issue 9: 23-30, DOI: 10.25236/AJCIS.2026.090904

A Traffic Flow Optimization Strategy for Ramp Merging Bottlenecks Based on Cooperative Control of Connected and Automated Vehicles

Mingyu Jiang*

School of Transportation and Logistics, Southwest Jiaotong University, Chengdu, China
1403224326@qq.com
**Corresponding author*

Abstract: *Ramp merging areas are a persistent bottleneck of urban expressways: on-ramp vehicles compete with the mainline stream for the same gaps, the resulting deceleration propagates upstream, and stop-and-go behaviour raises both delay and fuel consumption. Connected and automated vehicles (CAVs) can exchange state information with surrounding vehicles and with roadside infrastructure, which makes the merging manoeuvre controllable instead of dependent on individual gap acceptance. This paper develops a two-layer cooperative merging strategy for a single-lane mainline and a single-lane on-ramp on which all vehicles are CAVs. The first layer formulates the merging sequence as a mixed-integer program that minimises the total time at which the controlled vehicles clear the merge point under vehicle dynamics and headway constraints. The second layer plans the longitudinal motion of each vehicle by optimal control with a weighted cost on acceleration and jerk, and the resulting trajectory is available in closed form for real-time execution. In simulations with balanced and unbalanced demand, the coupled strategy reduced average delay and raised mean speed relative to first-in-first-out and zipper merging, and cut fuel consumption by 12.56% and 12.90% at the highest demand, although it used slightly more fuel when demand was low.*

Keywords: *Ramp Merging Area, Connected and Automated Vehicles, Cooperative Control, Mixed Integer Programming, Optimal Control, Trajectory Optimization*

1. Introduction

Ramp merging areas are persistent bottlenecks of urban expressways: a vehicle entering from an on-ramp must occupy a gap in the mainline stream, and the resulting deceleration propagates upstream as a slow-moving wave. Driver-related factors dominate crash causation near the merge point [1].

Ramp metering restricts the inflow of on-ramp vehicles with local feedback laws such as ALINEA [2, 3], but it acts on demand rather than on the manoeuvre itself and leaves the merge uncoordinated.

Connected and automated vehicles (CAVs) can exchange state information with neighbouring vehicles and with roadside infrastructure, which makes the merging manoeuvre controllable. Centralized formulations plan the whole merging group under safety constraints [4-6], and Rios-Torres and Malikopoulos [7] reported lower fuel consumption for a first-in-first-out (FIFO) sequence. Field implementations include a vehicle-to-cloud system [8] and a fuzzy controller [9].

Distributed schemes trade optimality for communication load: ramp vehicles have been mapped onto the mainline as virtual vehicles [10], a unified longitudinal control law has been proposed [11], platoons and lanes have been assigned by vehicle-to-vehicle communication [12], and hierarchical and game-based formulations determine the sequence centrally or by cooperative bargaining [13, 14]. Most of these studies nevertheless optimize the sequence and the trajectories separately.

This paper couples the two decisions for a single-lane mainline and a single-lane on-ramp on which every vehicle is a CAV. The sequence is formulated as a mixed-integer program that minimizes the time at which the controlled vehicles clear the merge point under vehicle dynamics and headway constraints, and each trajectory is planned by optimal control that weights acceleration and jerk, in closed form.

ISSN 2616-5775 Vol. 9, Issue 9: 23-30, DOI: 10.25236/AJCIS.2026.090904

2. Framework of the Cooperative Merging Control Strategy

The merging area is a single-lane mainline connected to a single-lane on-ramp (Figure 1). Lane changing and overtaking are not permitted, so the merge point is fixed at the junction of the two lanes. Because the range of a roadside unit (RSU) is limited the approach is divided into a cooperative control zone and a merging zone; the zone length L is the distance from its upstream boundary to the merge point.

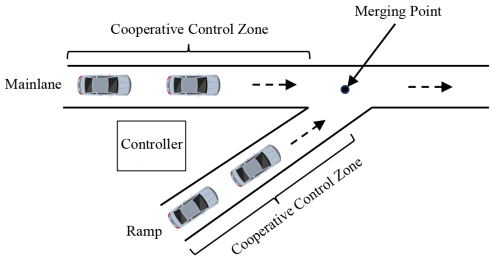


Figure 1: Layout of the studied merging area, showing the cooperative control zone, the merging zone and the merge point.

Each vehicle carries an on-board unit supporting vehicle-to-vehicle and vehicle-to-infrastructure communication. When a vehicle enters the control zone the RSU reads its state and forwards the arrival sequence to the traffic management centre, which returns a control plan delivered before the merge point. The first layer decides the order in which the controlled vehicles pass the merge point (Section 3) and the second plans each trajectory (Section 4).

3. Merging Sequence Optimization Based on Mixed Integer Programming

The first layer determines when each controlled vehicle should pass the merge point. It is formulated as a mixed-integer program because the priority between two vehicles is discrete while the passage times are continuous, and it is built from the merging rules, the safety constraints and the objective.

3.1. Merging Rules and Potential Sequences

Several rules decide which vehicle merges first. Mainline priority protects the mainline stream when its speed is much higher than the ramp speed, and zipper merging alternates vehicles from the two links but requires drivers to observe the other link. First-in-first-out (FIFO) merging keeps the arrival order, which is natural where overtaking is impossible, but it wastes merging opportunities and increases delay [7].

Once the arrival order is known, every order in which the vehicles can leave the merge point is a potential sequence. Figure 2 shows the simplest case, in which two mainline vehicles M1 and M2 and one ramp vehicle R1 enter the control zone; three departure sequences are possible. The problem is therefore rewritten as a timetable over the times at which the controlled vehicles reach the merge point.

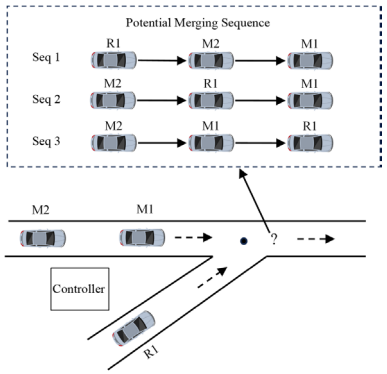


Figure 2: Potential merging sequences for two mainline vehicles (M1, M2) and one ramp vehicle (R1) entering the control zone in the order M1-R1-M2.

ISSN 2616-5775 Vol. 9, Issue 9: 23-30, DOI: 10.25236/AJCIS.2026.090904

3.2. Optimization Model and Solution Procedure

The decision variables are the passage times of the controlled vehicles and a binary variable b that assigns priority between two vehicles arriving from different lanes. With n_1 mainline and n_2 ramp vehicles the priority decisions are stored in a matrix B, and the objective is the total time that the controlled vehicles need to clear the merge point, Eq. (1).

$$\min_{t,B} \sum_{i=1}^{n} (t_i^f - t_i^0) \tag{1}$$

where t_i^f is the time at which vehicle i reaches the merge point (s), t_i^0 is the time at which the vehicle enters the control zone (s), n is the number of controlled vehicles, and B is the matrix of priority decisions.

Every vehicle must cross the control zone within the performance limits of the vehicle and the road. Between its entry and the merge point it either accelerates to the maximum speed and then cruises or accelerates over the whole interval, so the shortest crossing time without interference depends on the zone geometry and the dynamic limits, Eq. (2).

$$t_i^{\min} = t_i^0 + \min\left(\frac{\sqrt{(v_i^0)^2 + 2a_{\max}L - v_i^0}}{a_{\max}}, \frac{v_{\max} - v_i^0}{a_{\max}}, \frac{v_{\max} - v_i^0}{a_{\max}} + \frac{2a_{\max}L - v_{\max}^2}{2a_{\max}v_{\max}} \right) \tag{2}$$

where $v_{\max}$ is the maximum speed allowed on the link (m/s), $a_{\min}$ is the maximum acceleration (m/s²), $d_{\min}$ is the comfortable deceleration (m/s²) and L is the length of the cooperative control zone (m).

The shortest time is attainable for the first vehicle that enters the control zone. For every following vehicle the interference of the preceding vehicle makes the actual passage time larger, as expressed by Eq. (3), in which h_d is the minimum headway maintained between two successive vehicles at the merge point.

$$t_i^f \geq \max\{t_{i-1}^f + h_d, t_i^{\min}\}, \forall i \in \mathbf{N} \tag{3}$$

The headway requirement covers the two arrival cases. In the first case the two vehicles enter the control zone on the same lane, as shown in Figure 3: overtaking is not allowed, so the leading vehicle passes the merge point first and Eq. (4) requires the headway between them to exceed the threshold h_1.

$$t_i^f - t_{i-1}^f \geq h_1, \forall i \in \mathbf{S} \tag{4}$$

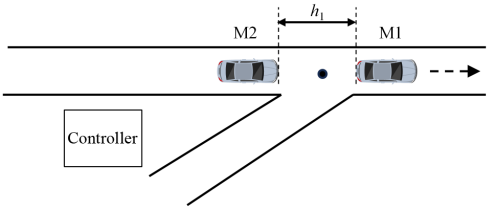


Figure 3: Headway constraint for two vehicles entering the control zone on the same lane.

In the second case the two vehicles arrive from different lanes, as shown in Figure 4. Because the lateral manoeuvre is not modelled explicitly a larger threshold h_2 covers the lateral conflict as well, and the resulting constraint is Eq. (5).

$$\left| t_k^f - t_l^f \right| \geq h_2, \forall k, l \in \mathbf{D} \tag{5}$$

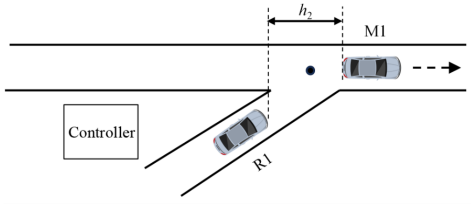


Figure 4: Headway constraint for two vehicles entering the control zone from different lanes.

ISSN 2616-5775 Vol. 9, Issue 9: 23-30, DOI: 10.25236/AJCIS.2026.090904

Eq. (5) is enforced in the direction selected by the binary variable: Eq. (6) when $b = 0$ and Eq. (7) when $b = 1$, where the constant M is large enough to deactivate the inequality that does not correspond to the chosen priority.

$$t_k^f - t_l^f + b_{k,l} \times M \geq h_2, \forall k, l \in \mathbf{D} \tag{6}$$

$$t_l^f - t_k^f + (1 - b_{k,l}) \times M \geq h_2, \forall k, l \in \mathbf{D} \tag{7}$$

The two cases cover all arrival combinations, so any sequence that satisfies the constraints is safe with respect to the longitudinal motion. The model assumes a straight, level road and identical vehicles.

The RSU numbers the CAVs in arrival order and the controller solves the mixed-integer program, which returns the merging timetable. That timetable is passed to the trajectory layer of Section 4, and the average delay in the merging area is used in Section 5.

4. Trajectory Optimization Based on Optimal Control

Once the sequence model has fixed the time at which each vehicle should reach the merge point, the trajectory layer controls the intermediate motion so that it complies with that timetable, as an optimal control problem whose cost combines fuel consumption and ride comfort and is solved analytically.

4.1. Trajectory Optimization Model

The trajectory is chosen to minimize the quadratic cost of Eq. (8), in which the weights w_1 and w_2 set the trade-off between fuel consumption and ride comfort: a small weight on jerk allows abrupt changes of acceleration, whereas an excessive weight produces an aggressive input.

$$\min_{u_i} \frac{1}{2} \int_{t_0}^{t_f} (\omega_1 a_i(t)^2 + \omega_2 u_i(t)^2)\, dt \tag{8}$$

where w_1 and w_2 are the weights of the acceleration term and the jerk term, respectively.

The motion is subject to the physical limits of the road and of the vehicle: Eqs. (9) to (12) bound the speed, the acceleration and the jerk over the interval from entry into the control zone to the merge point.

$$v_{\min} \leq v_i \leq v_{\max} \tag{9}$$

$$a_{\min} \leq a_i \leq a_{\max} \tag{10}$$

$$u_{\min} \leq u_i \leq u_{\max} \tag{11}$$

$$t \in [t_0, t_f] \tag{12}$$

where $v_{\max}$ and $v_{\min}$ are the maximum and minimum speeds of the link (m/s), $a_{\max}$ and $a_{\min}$ are the maximum acceleration and the minimum deceleration of the vehicle (m/s²), $u_{\max}$ and $u_{\min}$ are the bounds on the jerk (m/s³), and t_0 and t_f are the times at which the vehicle enters the control zone and reaches the merge point.

Solving the optimal control problem numerically is too slow for a real-time controller. Because the sequence model already guarantees that the intermediate states remain inside the dynamic limits the problem is treated as unconstrained and solved analytically: Eqs. (13) to (16) give the jerk, acceleration, speed and position of vehicle i, in which the six integration constants c_1 to c_6 are the same in all four expressions.

$$u_i^*(t) = c_3 \sqrt{\frac{\omega_1}{\omega_2}} e^{\sqrt{\frac{\omega_1}{\omega_2}}t} - c_4 \sqrt{\frac{\omega_1}{\omega_2}} e^{-\sqrt{\frac{\omega_1}{\omega_2}}t} + \frac{c_1}{\omega_1} \tag{13}$$

$$a_i^*(t) = c_3 e^{\sqrt{\frac{\omega_1}{\omega_2}}t} + c_4 e^{-\sqrt{\frac{\omega_1}{\omega_2}}t} + \frac{c_1}{\omega_1} t - \frac{c_2}{\omega_2} \tag{14}$$

$$v_i^*(t) = c_3 \sqrt{\frac{\omega_2}{\omega_1}} e^{\sqrt{\frac{\omega_1}{\omega_2}}t} - c_4 \sqrt{\frac{\omega_2}{\omega_1}} e^{-\sqrt{\frac{\omega_1}{\omega_2}}t} + \frac{1}{2}\frac{c_1}{\omega_1} t^2 - \frac{c_2}{\omega_2} t + c_5 \tag{15}$$

ISSN 2616-5775 Vol. 9, Issue 9: 23-30, DOI: 10.25236/AJCIS.2026.090904

$$p_i^*(t) = c_3\frac{\omega_2}{\omega_1}e^{\sqrt{\frac{\omega_1}{\omega_2}}t} + c_4\frac{\omega_2}{\omega_1}e^{-\sqrt{\frac{\omega_1}{\omega_2}}t} + \frac{1}{6}\frac{c_1}{\omega_1}t^3 - \frac{1}{2}\frac{c_2}{\omega_2}t^2 + c_5t + c_6 \tag{16}$$

where c_1 to c_6 are the integration constants of the closed-form solution.

The integration constants follow from the boundary conditions: substituting the known initial state and the merge time imposed by the sequence model into Eqs. (14) to (16) gives a linear system for c_1 to c_6.

4.2. Fuel Consumption Model

The cost of Eq. (8) represents ride comfort, while the fuel consumed is estimated from a cruise component and an acceleration component [15]: Eq. (17) is a cubic polynomial in speed and Eq. (18) is proportional to the apparent acceleration. The coefficients b_0 to b_3 and c_0 to c_2 are fitted from measured data and the total rate of fuel consumption is their sum, Eq. (19).

$$f_{cruise} = b_0 + b_1v + b_2v^2 + b_3v^3 \tag{17}$$

$$f_{accel} = \hat{a}(c_0 + c_1v + c_2v^2) \tag{18}$$

$$f_v = f_{cruise} + f_{accel} \tag{19}$$

where v is the vehicle speed (m/s) and a is the apparent acceleration (m/s²). Because the road is level the apparent acceleration is produced by the engine alone, and fuel injection is cut off during braking.

5. Simulation Analysis

The strategy was implemented in Python 3.11.8, and the mixed-integer program was solved with Gurobi 11.0.0 on a Windows 11 computer with an Intel Core i9-13980HX processor. Two baselines were used for comparison: a centralized FIFO strategy [7] and zipper merging. Unless stated otherwise, 50 mainline and 50 ramp CAVs entered the control zone at an arrival rate of 0.25 veh/s on each link, which is the balanced demand case, and the weights of the performance index were set to $w_1 = w_2 = 0.5$.

5.1. Merging Sequence and Trajectory Results

Figure 5 shows the position-time trajectories of the controlled vehicles under the three strategies, with the mainline vehicles plotted above the axis and the ramp vehicles below; the intersection of a trajectory with the axis marks when that vehicle completes merging. The proposed strategy delays or advances neighbouring vehicles within the safety constraints so that one link passes the merge point in groups.

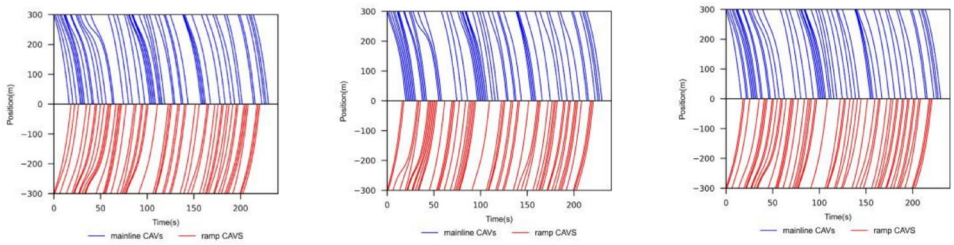


Figure 5: Position-time trajectories of the controlled vehicles under (a) zipper merging, (b) the proposed strategy and (c) FIFO merging, with mainline vehicles above and ramp vehicles below the axis.

All three strategies use the same optimal control layer, so the differences in Figure 6 originate from the sequence alone: ramp vehicles are held behind the mainline group and then accelerate, and the fifth mainline vehicle slows down so that the ramp platoon can pass. The speed stays inside the limits of the link, the acceleration remains between -0.5 m/s² and 2.5 m/s², and the jerk stays smooth.

ISSN 2616-5775 Vol. 9, Issue 9: 23-30, DOI: 10.25236/AJCIS.2026.090904

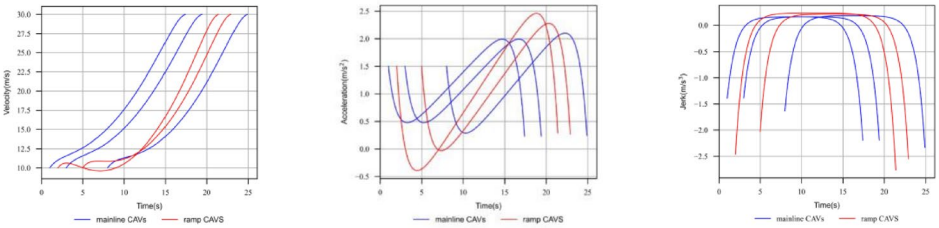


Figure 6: Trajectories of five selected vehicles under balanced demand: (a) velocity, (b) acceleration and (c) jerk under the proposed strategy.

5.2. Performance under Balanced and Unbalanced Demand

The strategy was evaluated with the average delay, mean speed and fuel consumption of the controlled vehicles. The average delay is the difference between the time at which a vehicle actually completes merging and the shortest time in which it could have done so, averaged over all n vehicles, Eq. (20).

$$d_{avg} = \frac{1}{n}\sum_{i=1}^{n}(t_i^f - t_i^{\min}) \tag{20}$$

where n is the number of controlled vehicles, t_i^f is the time at which vehicle i actually completes merging (s), and $t_i^{\min}$ is the shortest time in which vehicle i could have completed merging (s).

Under balanced demand the proposed strategy reduced the average delay of both the mainline and the ramp by about 44% relative to the two baselines (Figure 7). FIFO must respect the arrival order and zipper merging forces one link to yield, so both waste merging opportunities.

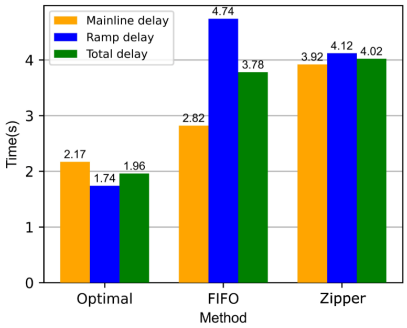


Figure 7: Average delay of the mainline, the ramp and the whole merging area under the proposed strategy, FIFO merging and zipper merging at balanced demand.

The three strategies share the same terminal speed because they use the same optimal control layer. In the proposed strategy the interquartile range of the vehicle speeds is concentrated near that maximum, whereas zipper merging produces a wider spread (Figure 8).

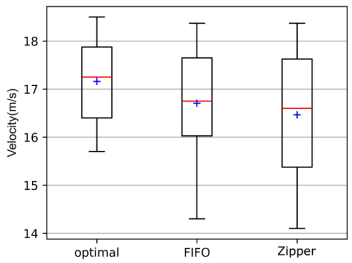


Figure 8: Distribution of vehicle speeds under the proposed strategy, FIFO merging and zipper merging at balanced demand.

At this demand level the proposed strategy consumed slightly more fuel than the two baselines (Figure 9), because its higher speeds raise the speed and acceleration terms of the fuel model while the decelerations of the baselines do not develop into congestion.

ISSN 2616-5775 Vol. 9, Issue 9: 23-30, DOI: 10.25236/AJCIS.2026.090904

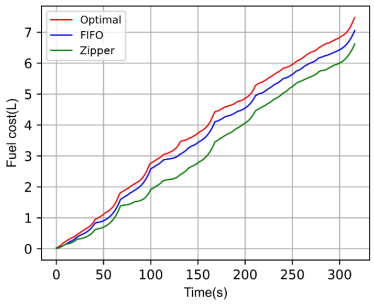


Figure 9: Cumulative fuel consumption of the three strategies at balanced demand.

The demand was then varied to reproduce the unbalanced condition of a real expressway. Three combinations were simulated for five minutes each, from 800 pcu/h on the mainline with 300 pcu/h on the ramp to 1500 pcu/h with 900 pcu/h; Table 1 collects the resulting delay, mean speed and fuel consumption.

Table 1: Delay, mean speed and fuel consumption of the three strategies under unbalanced demand.

Demand (pcu/h)	Strategy	Mainline average delay (s)	Ramp average delay (s)	Average delay (s)	Average speed (m/s)	Fuel consumption (L)
Mainline 800 / ramp 300	Proposed strategy	0.2448	0.4018	0.2882	17.8	8.2798
	FIFO merging	0.2543	0.4186	0.2997	17.2	8.0319
	Zipper merging	0.5979	0.1610	0.4771	16.9	8.1787
Mainline 1200 / ramp 600	Proposed strategy	0.4779	0.4921	0.4827	16.9	8.9314
	FIFO merging	0.4286	0.6824	0.6742	16.4	9.8245
	Zipper merging	1.3132	0.4967	1.0393	16.1	10.7651
Mainline 1500 / ramp 900	Proposed strategy	0.8196	0.9202	0.8574	16.8	16.5247
	FIFO merging	1.4360	1.9002	1.6107	15.8	18.8983
	Zipper merging	2.1521	1.1570	1.7776	15.5	19.0274

Delay increased with demand for all three strategies, because two links with similar arrival rates admit more admissible sequences and are therefore easier to coordinate. As demand grows, FIFO and zipper merging waste merging opportunities and queues on the mainline become longer, whereas the proposed strategy keeps the highest mean speed. At the highest demand the proposed strategy saved 12.56% and 12.90% of fuel relative to FIFO and zipper merging respectively.

6. Conclusions

This paper developed a two-layer cooperative control strategy for ramp merging bottlenecks with connected and automated vehicles: the merging sequence is formulated as a mixed-integer program that minimizes the time at which the controlled vehicles clear the merge point, and each trajectory is planned by optimal control with a weighted cost on acceleration and jerk.

Simulation with balanced and unbalanced demand showed that the strategy reduced the average delay by about 44% in the balanced case, maintained the highest mean speed in every demand condition, and saved 12.56% and 12.90% of fuel at the highest demand, although it consumed slightly more fuel than the baselines when demand was low.

Two limitations bound these results. The model represents a single-lane mainline, so lateral lane changing and its interaction with the merging sequence are not covered. The sequence model is also solved centrally, so its computation time limits the size of the control zone.

References

[1] Singh, S. (2015) Critical Reasons for Crashes Investigated in the National Motor Vehicle Crash Causation Survey. Traffic Safety Facts, Crash Stats.

[2] Hadj-Salem, H., Blosseville, J.M. and Papageorgiou, M. (1990) ALINEA: A Local Feedback Control Law for On-Ramp Metering; A Real-Life Study. Third International Conference on Road Traffic Control, 194-198.

ISSN 2616-5775 Vol. 9, Issue 9: 23-30, DOI: 10.25236/AJCIS.2026.090904

[3] Papageorgiou, M. and Kotsialos, A. (2002) Freeway Ramp Metering: An Overview. IEEE Transactions on Intelligent Transportation Systems, 3(4), 271-281. https://doi.org/10.1109/TITS.2002.806803

[4] Raravi, G., Shingde, V. and Ramamritham, K. (2007) Merge Algorithms for Intelligent Vehicles. In: Ramesh, S. and Sampath, P. (eds.) Next Generation Design and Verification Methodologies for Distributed Embedded Control Systems, 51-65. Springer, Dordrecht. https://doi.org/10.1007/978-1-4020-6254-4_5

[5] Awal, T., Kulik, L. and Ramamohanrao, K. (2013) Optimal Traffic Merging Strategy for Communication- and Sensor-Enabled Vehicles. 16th International IEEE Conference on Intelligent Transportation Systems, 1468-1474. https://doi.org/10.1109/ITSC.2013.6728437

[6] Ntousakis, I.A., Nikolos, I.K. and Papageorgiou, M. (2016) Optimal Vehicle Trajectory Planning in the Context of Cooperative Merging on Highways. Transportation Research Part C: Emerging Technologies, 71, 464-488. https://doi.org/10.1016/j.trc.2016.08.007

[7] Rios-Torres, J. and Malikopoulos, A.A. (2017) Automated and Cooperative Vehicle Merging at Highway On-Ramps. IEEE Transactions on Intelligent Transportation Systems, 18(4), 780-789. https://doi.org/10.1109/TITS.2016.2587582

[8] Liao, X., Wang, Z., Zhao, X., et al. (2022) Cooperative Ramp Merging Design and Field Implementation: A Digital Twin Approach Based on Vehicle-to-Cloud Communication. IEEE Transactions on Intelligent Transportation Systems, 23(5), 4490-4500. https://doi.org/10.1109/TITS.2020.3045123

[9] Milanés, V., Godoy, J., Villagrá, J., et al. (2011) Automated On-Ramp Merging System for Congested Traffic Situations. IEEE Transactions on Intelligent Transportation Systems, 12(2), 500-508. https://doi.org/10.1109/TITS.2010.2096812

[10] Uno, A., Sakaguchi, T. and Tsugawa, S. (1999) A Merging Control Algorithm Based on Inter-Vehicle Communication. Proceedings of the 1999 IEEE/IEEJ/JSAI International Conference on Intelligent Transportation Systems, 783-787. https://doi.org/10.1109/ITSC.1999.821160

[11] Lu, X.Y. and Hedrick, J.K. (2003) Longitudinal Control Algorithm for Automated Vehicle Merging. International Journal of Control, 76(2), 193-202. https://doi.org/10.1080/0020717031000079418

[12] Dao, T.S., Clark, C.M. and Huissoon, J.P. (2008) Distributed Platoon Assignment and Lane Selection for Traffic Flow Optimization. 2008 IEEE Intelligent Vehicles Symposium, 739-744. https://doi.org/10.1109/IVS.2008.4621202

[13] Ran, B., Leight, S. and Chang, B. (1999) A Microscopic Simulation Model for Merging Control on a Dedicated-Lane Automated Highway System. Transportation Research Part C: Emerging Technologies, 7(6), 369-388. https://doi.org/10.1016/S0968-090X(99)00028-5

[14] Jing, S., Hui, F., Zhao, X., et al. (2019) Cooperative Game Approach to Optimal Merging Sequence and On-Ramp Merging Control of Connected and Automated Vehicles. IEEE Transactions on Intelligent Transportation Systems, 20(11), 4234-4244. https://doi.org/10.1109/TITS.2019.2925871

[15] Kamal, M.A.S., Mukai, M., Murata, J. and Kawabe, T. (2011) Ecological Vehicle Control on Roads With Up-Down Slopes. IEEE Transactions on Intelligent Transportation Systems, 12(3), 783-794. https://doi.org/10.1109/TITS.2011.2112648